NJC
New Journal of Chemistry
A journal for new directions in chemistry

Accepted Manuscript

This article can be cited before page numbers have been issued, to do this please use: L. Yin, C. Yang, Y. Han, H. Zhang, F. Jiang, W. Zhong, C. Gong and Q. Tang, *New J. Chem.*, 2025, DOI: 10.1039/D5NJ02611C.

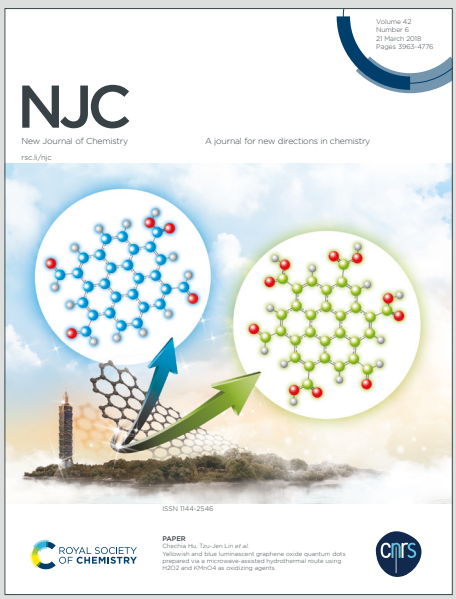

View Article Online
DOI: 10.1039/D5NJ02611C

ARTICLE

A semi-solid hydrogel state electrochromic device based on asymmetric disubstituted viologen containing a quaternary ammonium group with enhanced electrochromic stability

Received 00th January 20xx,
Accepted 00th January 20xx

DOI: 10.1039/x0xx00000x

Lin Yin, Chen-xin Yang, Yu-xuan Han, Hao Zhang, Feng-lu Jiang, Wen-tao Zhong, Cheng-bin Gong* and Qian Tang*

This work aims to investigate the electrochromic behavior of an asymmetric disubstituted viologen containing a quaternary ammonium group in semi-solid hydrogel state electrochromic devices. An asymmetric disubstituted viologen **BTMAPP^{3+}3Br$^-$** was synthesized as the electrochromic material, and two symmetric disubstituted viologens (**DTMAPP^{4+}4Br$^-$** and **DBP^{2+}2Br$^-$**) were synthesized as the control electrochromic materials. Polyacrylamide hydrogel state ECDs based on three electrochromic materials were assembled by in-situ photo-initiated polymerization of acrylamide under UV light, and their electrochemical and electrochromic performance were investigated. They showed similar electrochemical performance. They also required a same working voltage and achieved a similar color change from colorless bleached state to blue-purple colored state. It's noteworthy that the ECD based on **BTMAPP^{3+}3Br$^-$** showed a better cycling stability (retaining of the initial optical contrast after 16,000 s monitored: 95.6% versus 70.7% and 78.5%) and a higher coloration efficiency (115 cm^2/C versus 96 cm^2/C and 103 cm^2/C) compared to the PAM ECDs based on two symmetric disubstituted viologen. The results indicate that an asymmetric disubstituted viologen containing a quaternary ammonium group can enhance the cycling stability of the gel-state ECD through suppressing the formation of radical cation dimers. The all-in-one semi-solid hydrogel state ECDs based on **BTMAPP^{3+}3Br$^-$** with advantages of easy-to-make process, good cycling stability, low operating voltage, high coloration efficiency and low power consumption offer a new choice for electronic labels, solar cell powered displays, smart windows, etc..

Introduction

As energy sources are increasingly depleted, the development of energy-saving techniques has become a focal point. Electrochromic devices (ECDs) based on electrochromic materials (ECMs) can reversibly change their optical properties (absorbance, transmittance, color) under an electrical stimulation.[1,2] ECDs are widely used in smart windows,[3-5] displays,[5,6] camouflage[7,8] and supercapacitors[9,10] due to their energy-saving advantage and rich color change.

The performance of an ECD is highly dependent on the ECM. In general, ECMs include inorganic and organic materials, both have their own advantages. Because of the advantages of good redox stability, low applied voltage and rich color changes, viologens are the most widely studied organic ECMs since Schoot et al. reported its electrochromic behavior in ECD for the first time in 1973.[11-13] The electrochromic performance of viologens is related to the N-substituents. Although symmetric disubstituted viologens show better cycling stability compared to monosubstituted viologens, poor cycling stability during cycle process often occurs on symmetric disubstituted viologens due to the formation of viologen radical cation dimers, this greatly limits their practical applications. The introduction of π-spacer can effectively enhance electrochromic properties of viologens, but this often causes the requirement of a higher working voltage.[2,14] Kim et al.[15] found that an asymmetric disubstituted viologen with two different N-substituents (1-benzyl-1'-heptyl-4,4'-bipyridinium salt) could suppress dimer formation in liquid-state ECD, which showed better cycling stability compared to a symmetric disubstituted viologen with same N-substituents (1,1'-diheptyl-4,4'-bipyridinium salt). In addition, Ambrose et al.[16] and Ben et al.[17] utilized viologen derivatives containing quaternary ammonium groups as the electroactive material of the negative electrolyte in redox flow batteries, they found the introduction of quaternary ammonium groups could enhance the solubility and diminish the radical dimerization and thus enhance its stability.

Inspired by their work, we speculate whether an asymmetric disubstituted viologen containing a quaternary ammonium group can further enhance the cycling stability of the ECD. To illustrate this, an asymmetric viologen with two different N-substituents (butyl and (3-trimethylammonio)propyl) and a quaternary ammonium group, **BTMAPP^{3+}3Br$^-$**, was designed as the ECM (Scheme 1). For a comparison, two symmetric disubstituted viologens, **DBP^{2+}2Br$^-$** with two same N-

The Key Laboratory of Applied Chemistry of Chongqing Municipality, College of Chemistry and Chemical Engineering, Southwest University, Chongqing, 400715, P. R. China. E-mail: gongcbtq@swu.edu.cn (C. -b Gong), *qiantang@swu.edu.cn* (Q. Tang)

† Supplementary Information available. See DOI: 10.1039/x0xx00000x

View Article Online DOI: 10.1039/D5NJ02611C

substituents of butyl and **DTMAPP^{4+}4Br^{-}** with two same N-substituents of (3-trimethylammonio)propyl), were also synthesized as control ECMs (Scheme 1).

As gel-state ECDs possess the advantages of solid- and liquid-state ECDs, therefore they are considered to have great development prospects.[18] In general, the gel electrolytes of gel-state ECDs can be divided into polymer-based organic gels and hydrogels. Organic gels are generally prepared by dispersing organic polymers (e.g., poly(methyl methacrylate),[19] polyvinyl butyral,[20] polyvinyl formal,[21] etc.) into high boiling organic solvents (e.g., propylene carbonate, diethylene glycol monobutyl ether, 1-mentyl-2-pyrrolidinone, etc.). However, organic solvents are difficult to degrade in natural, so more environmentally friendly hydrogels with water as the solvent become a better choice. At present, the hydrogel systems include carboxymethylcellulose sodium,[18,22.23] sodium carboxymethyl chitosan,[24] polyvinyl alcohol (PVA)-borax [1,25,26] and polyacrylamide (PAM)[18,27,28]. However, these hydrogels need to be coated on ITO glass after curing, which not only increases the production process of ECDs but also brings problem of bubbles by stirring and uneven coating. It's worth to note that PAM hydrogel can be prepared by in-situ polymerization of the monomer acrylamide (AM) under UV light, where the precursor solution is injected into the ECD frame in advance, thus overcomes these shortcomings. Meanwhile, the PAM hydrogel with a high concentration of LiCl can bring a high ionic conductivity and show excellent water retention capacity, it's an idea electrochromic hydrogel matrix.

In this work, all-in-one PAM hydrogel-state ECDs were constructed to investigate the electrochromic performance of **BTMAPP^{3+}3Br^{-}** and two control ECMs. All three ECDs achieved a similar color change from colorless bleached state to blue-purple colored state. In PAM ECDs, **BTMAPP^{3+}3Br^{-}** showed one pair of redox peaks and a lower diffusivity than **DTMAPP^{4+}4Br^{-}** and **DBP^{2+}2Br^{-}.** As expected, **BTMAPP^{3+}3Br^{-}** showed better cycling stability, the cycling stability decreased as the order: **BTMAPP^{3+}3Br^{-}** < **DTMAPP^{4+}4Br^{-}**< **DBP^{2+}2Br^{-}**. In addition, **BTMAPP^{3+}3Br^{-}** had a higher coloration efficiency than **DTMAPP^{4+}4Br^{-}** and **DBP^{2+}2Br^{-}**. The results indicate that an asymmetric disubstituted viologen containing a quaternary ammonium group can enhance the cycling stability of the hydrogel-state ECD through suppressing the formation of radical cation dimers. The all-in-one gel-state ECD based on **BTMAPP^{3+}3Br^{-}** with advantages of easy-to-make process, low operating voltage, moderate coloration efficiency and optical contrast, good cycling stability and low power consumption, the applications in electronic label, solar cell powered displays and smart windows were explored, indicating its promising in energy-saving fields.

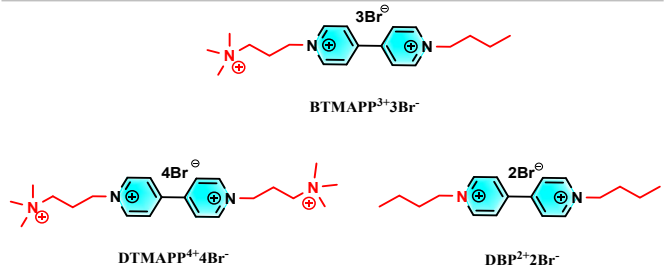

Scheme 1. Chemical structures of **BTMAPP^{3+}3Br^{-}**, **DTMAPP^{4+}4Br^{-}** and **DBP^{2+}2Br^{-}.**

Results and discussion

The internal resistance and ionic conductivity of PAM hydrogels with different LiCl concentrations were measured by EIS. As illustrated in Fig. 1a, all EIS curves exhibited a linear trend, this demonstrates that ionic conductivity within the PAM hydrogels is a non-faradaic process without any species or charges traversing the electrode-conductor interface.[29] Ionic conductivity was calculated using Equation (1):

$$\sigma = \frac{\mathrm{d}}{\mathrm{R_S \times S}} \times 1000 \qquad (1)$$

where σ represents the ionic conductivity (mS/cm), d and S denote the thickness (0.05 cm) and effective area (3 × 3 cm^2), and R_s represents the internal resistance (Ω) which is obtained from the intercept of the high frequency curve in the AC impedance spectrum with the horizontal axis.

The R_s values of PAM_1, PAM_2, PAM_3, PAM_4, PAM_5 and PAM_6 hydrogels were measured to be about 4.32, 2.73, 0.82, 0.53, 0.47 and 0.46 Ω, respectively. As illustrated in Fig. 1b, the ionic conductivities of PAM_1, PAM_2, PAM_3, PAM_4, PAM_5 and PAM_6 were calculated as 1.3, 2.0, 6.8, 10.5, 11.8 and 12.1 mS/cm, respectively. Namely, the ionic conductivity showed an increasing trend as the LiCl concentration increased. At the beginning, the ionic conductivity markedly increased as LiCl concentration increased, when it reached 2.00 mol/L, the rate slowed down, and almost saturated at 4.00 mol/L. Therefore, PAM_4 hydrogel with a LiCl concentration of 2.00 mol/L was chosen as the optimal hydrogel considering economy.

The transmittance of a hydrogel is an important parameter to judge whether it can be used as the electrolytes for ECDs. The transmittances of PAM_4 hydrogel, PAM_4 precursor solution and ITO glass were measured by UV-Vis (Fig. 1c), where the hydrogel and precursor solution with a size of 3 cm × 3 cm × 0.05 cm were sandwiched between two pieces of ITO glass. The transmittance of the polymerized gel was close to that of the precursor solution with a high transmittance in the visible region (70%-82%), which was only slightly lower than that of a piece of ITO glass (77%-89%). The PAM_4 hydrogel film stripped from the ITO glass was transparent and colorless, the flower left behind it was clearly displayed (Inset in Fig. 1c).

Water decomposition voltage is an important parameter for hydrogel-state ECDs, the operation voltage window of PAM_4 was obtained by LSV (Fig. 1d). The theoretical decomposition voltage of water is 1.23 V,[30] which markedly limits its application in hydrogel-state ECDs. The PAM_4 hydrogel had a broader operating voltage window (0.0~1.5 V) compared to water, this may be due to the microporous structure of the polymer network, which effectively inhibits the movement of water molecules. To avoid the degradation of electrochromic properties caused by water decomposition, the subsequent

View Article Online
DOI: 10.1039/D5NJ02614D

measurement for electrochemical and electrochromic behaviors were all within the range of -1.5 ~ 1.5 V.

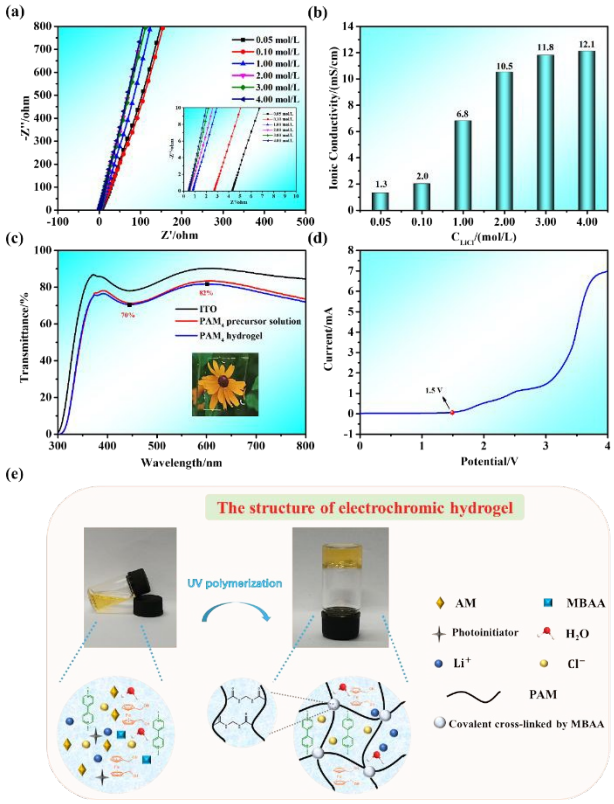

Fig. 1. Electrochemical impedance spectra (a) and ionic conductivity (b) of PAM hydrogels with different LiCl concentrations. Transmittance curves of PAM_4 precursor solution and PAM_4 hydrogel, Insets: PAM_4 hydrogel film stripped from ITO glass with a flower behind it (c). LSV curve of PAM_4 hydrogel (d). Schematic illustration of the preparation of electrochromic hydrogel based on PAM_4 (e).

With the advantages of high ionic conductivity, high transmittance and a wide operating window range, PAM_4 is suitable to serve as the hydrogel matrix of gel-state ECDs.

The electrochromic precursor solution based on PAM_4 was light yellow due to the introduction of $Fc(CH_2OH)_2$ as the complementary redox material, yellow electrochromic hydrogel was successfully obtained after irradiation with UV light, this indicates that the presence of the ECM, $Fc(CH_2OH)_2$ and the photoinitiator would not interfere UV-initiated polymerization (Fig. 1e). The ECM, $Fc(CH_2OH)_2$ and LiCl were dissolved in the micropores of PAM hydrogel covalently cross-linked by MBAA. PAM ECDs were easily assembled by sandwiching the electrochromic precursor solution between two pieces of ITO glass and subsequently irradiating with a UV light.

The redox behavior of PAM ECDs based on **BTMAPP^{3+}3Br$^-$**, **DTMAPP^{4+}4Br$^-$**, and **DBP^{2+}2Br$^-$** were studied by CV with a two-electrode system at a scanning speed of 100 mV/s. They all had two redox couples (Fig. 2), which is consistent with Zhao's research results.[25] The first redox couple at ca. 0.10/-0.10 V was attributed to the redox reaction of $Fc(CH_2OH)_2/[Fc(CH_2OH)_2]^+$ (Fig. S9). The second redox couple was assigned to redox reaction of **BTMAPP^{3+}/BTMAPP$^{2+\bullet}$**, **DTMAPP^{4+}/DTMAPP$^{3+\bullet}$** and **DBP^{2+}/DBP$^{+\bullet}$**, respectively, and the ratios of i_{pa}/i_{pc} were all close to 1, indicating that the electrochemical conversion is reversible. However, the CV curves of **BTMAPP^{3+}3Br$^-$**, **DTMAPP^{4+}4Br$^-$**, and **DBP^{2+}2Br$^-$** in H_2O had two pair of redox peaks (Fig. S10), this indicates that solvent environment can influence the electrochemical behavior of viologen. The reduction of cation radical to neutral state may require a voltage higher than -1.5 V in PAM hydrogel.[22] The redox peak potential data was recorded on Table S1, the E_{pc2} showed a decreasing trend with the increase of quaternary ammonium groups (-1.04 to -0.98 to -0.93 V), this is consistent with the research conclusion obtained by Beh et al..[17] This may be attributed to the electron-withdrawing characteristics of quaternary ammonium group, this will reduce the electron cloud density of the pyridine unit, thereby resulting in a greater electron deficiency in the pyridine unit and making it easier to get electron to be reduced.[23] The CV curve began to mutate around -0.75 V, accompanied by a reversible color change (colorless to blue-purple), indicating that **DBP^{2+}**, **DTMAPP^{4+}** and **BTMAPP^{3+}** began to be electrochemically reduced. The PAM ECDs were scanned by increasing the scanning rate from 50 mV/s to 300 mV/s, the results were shown in Fig. S11, both the anodic and cathodic peak currents showed a linear dependence on the square root of the scanning rate, this implies that redox reactions of **DBP^{2+}/DBP$^{+\bullet}$**, **DTMAPP^{4+}/DTMAPP$^{3+\bullet}$** and **BTMAPP^{3+}/BTMAPP$^{2+\bullet}$** are controlled by diffusion.[31] Compared to the PAM ECDs based on **DTMAPP^{4+}4Br$^-$** and **DBP^{2+}2Br$^-$**, the PAM ECD based on **BTMAPP^{3+}3Br$^-$** showed a lower diffusivity (Table S2), the results illustrate that radical dimerization is less likely to occur in the PAM ECD based on **BTMAPP^{3+}3Br$^-$**,[32] namely asymmetric disubstituted viologen could effectively suppress radical dimerization.

The UV-Vis absorption spectra of the PAM ECDs were measured in a two-electrode system upon application of external DC voltages. In PAM ECDs, $Fc(CH_2OH)_2$ served as a counter-electrode material to decrease the working voltage.[8] An ECM-free PAM ECD didn't undergo any changes in color and UV-Vis absorption spectrum upon application of 0.0 V and -1.5 V (Fig. S12), this indicates that the introduction of electrochemically active $Fc(CH_2OH)_2$ in PAM ECDs does not

View Article Online
DOI: 10.1039/D5NJ02611C

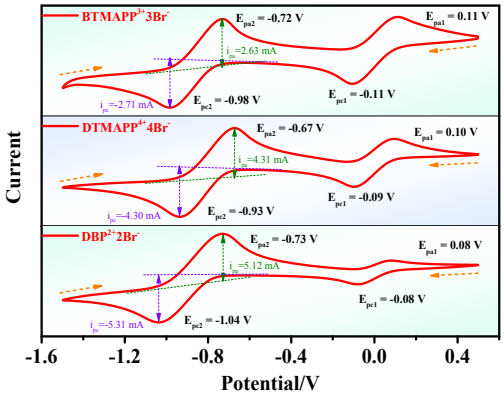

Fig. 2. Cyclic voltammogram curves of PAM ECDs based on **BTMAPP^{3+}3Br^{-}**, **DTMAPP^{4+}4Br^{-}** and **DBP^{2+}2Br^{-}** at a scanning speed of 100 mV/s.

affect the color and absorption spectrum. All the three PAM ECDs based on **BTMAPP^{3+}3Br^{-}**, **DBP^{2+}2Br^{-}**, and **DTMAPP^{4+}4Br^{-}** showed a similar optoelectronic properties (Fig. 3a and Fig. S13), PAM ECDs showed a colorless bleached state when the applied voltage was 0.0 V, and no new absorption bands appeared in the visible region when the applied voltage was gradually increased from 0.0 to -0.7 V in the negative direction. When the voltage was further increased to -0.8 V, a broad absorption band centered at about 550 nm or 553 nm appeared due to the transitions of **BTMAPP^{3+}**→**BTMAPP$^{2+\bullet}$**, **DBP^{2+}** → **DBP$^{+\bullet}$**, and **DTMAPP^{4+}** → **DTMAPP$^{3+\bullet}$**, and all three PAM ECDs showed a same colored state of blue-purple, the results are basically consistent with CV results. The absorption intensity increased as the applied voltage was further gradually increased and reached a saturation at -1.2 V, and the color of the ECD also gradually deepened. The chromaticity coordinates (L*a*b*) values of ECDs at bleached state (0.0 V) and colored state (-1.2 V) were shown in Table S3.

Cycling stability is an important parameter of ECDs, it can be obtained by monitoring the change in optical contrast during sequential switching. Optical contrast (ΔT) was defined as the difference in transmittance between the colored state and bleached state, it can be obtained by using equation (2):

$$\Delta T(\%) = T_{Bleached}(\%) - T_{Colored}(\%) \quad (2)$$

where $T_{Bleached}$ and $T_{Colored}$ represent the transmittance of ECD at bleached state and colored state, respectively. The

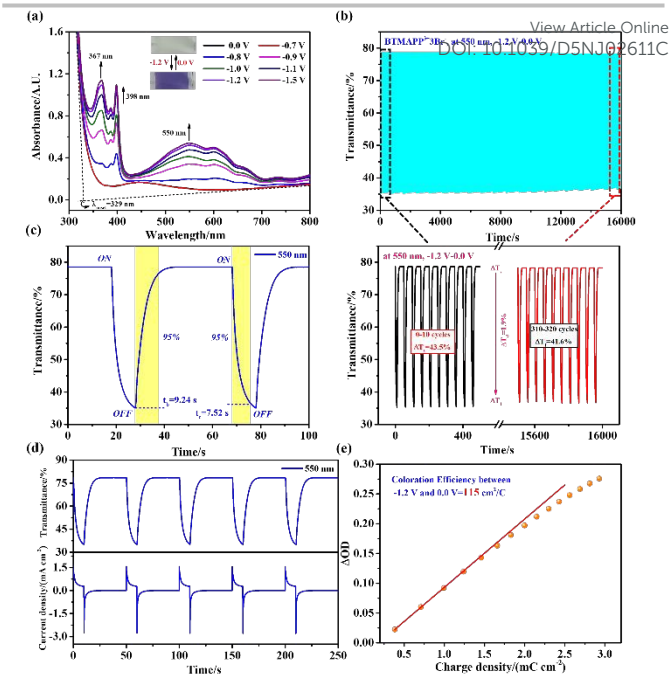

Fig. 3. Electrochromic properties of PAM ECD based on **BTMAPP^{3+}3Br^{-}**. UV-Vis absorption spectra at different applied voltages (a), electrochromic switching response (b), response time(c), chronoamperometry curve and the corresponding transmittance curve (d), and coloration efficiency (e) monitored between 0.0 V and -1.2 V at 550 nm. Insets in (a): photographs of the ECD at bleached state (0.0 V) and colored state (-1.2 V).

optical contrasts of PAM ECDs based on **DBP^{2+}2Br^{-}**, **DTMAPP^{4+}4Br^{-}** and **BTMAPP^{3+}3Br^{-}** were monitored at 550, 553 and 550 nm between -1.2 V and 0.0 V with a dwell time of 10 s and 40 s, respectively. As shown in Fig. 3b and Fig. S14, the ΔT_s of PAM ECDs based on **DBP^{2+}2Br^{-}**, **DTMAPP^{4+}4Br^{-}** and **BTMAPP^{3+}3Br^{-}** were 42.3%, 39.0% and 43.5%, respectively. The ΔT_s values of three PAM ECDs were comparable, but they showed different cycling stability. After 16,000 s (320 cycles), the retaining of the initial optical contrast was 70.7%, 78.5% and 95.6% for PAM ECDs based on **DBP^{2+}2Br^{-}**, **DTMAPP^{4+}4Br^{-}** and **BTMAPP^{3+}3Br^{-}**, respectively. The ECD based on **BTMAPP^{3+}3Br^{-}** exhibited the best cycling stability. For the ECDs based on viologens, it's well known that the optical contrast is highly dependent on the concentration of cation radical. Additionally, it was previously reported that the formation of dimeric species will cause the decrease of optical contrast during cycling.[12,13] Therefore, it was inferred that the formation of dimeric species is more difficult compared with the PAM ECDs based on symmetric **DBP^{2+}2Br^{-}** and **DTMAPP^{4+}4Br^{-}**, this may be due to its lower diffusivity as observed in CV results. Therefore, its long-term stability was further investigated. As shown in Fig. S15, the retainings of the initial optical contrast were 90.8%, 82.3% and 72.4% after 30,000 s (600 cycles), 60,000 s (1,200 cycles) and 90,000 s (1800 cycles). The results indicate that the introduction of quaternary ammonium group endows viologens a better cycling stability, whereas an asymmetric disubstituted viologen containing a quaternary ammonium group achieves the best cycling stability through suppressing the formation of radical cation dimers.

Since the human eye cannot accurately judge how fast the color of the ECD changes, the change in transmittance is used instead. The response time is defined as the time required for transmittance change to reach 95% during the colored state and bleached state at a special wavelength.[33] the results was shown in Fig. 3c, Fig. S16 and Table 1, the response times of coloration (t_c)/bleaching (t_b) for PAM ECDs based on **DBP^{2+}2Br$^-$**, **DTMAPP^{4+}4Br$^-$** and **BTMAPP^{3+}3Br$^-$** were 7.65/6.75, 7.68/6.93 and 7.52/9.24 s, respectively. The response time of these three PAM ECDs is longer than that of liquid-ECDs,[14] which may be because there are fewer solvents in the PAM hydrogel and the conductivity is low.

Coloration efficiency (CE) is another key parameter to evaluate the performance of ECDs, it can be obtained with equations (3) and (4):[34,35]

$$\mathrm{CE} = \frac{\Delta OD}{Q_d} \quad (3)$$

$$\Delta OD = \log\left(\frac{T_{Bleached}}{T_{colored}}\right) \quad (4)$$

where ΔOD represents the optical density, and Q_d denotes the amount of injected/ejected charge per unit area. The CE values was measured by double-potential chronoamperometry between -1.2 V and 0.0 V using electrochemical workstation and spectral dynamics using UV-Vis spectrophotometer at 550 nm for **DBP^{2+}2Br$^-$** and **BTMAPP^{3+}3Br$^-$** and at 553 nm for **DTMAPP^{4+}4Br$^-$**. Fig. 3d and Fig. S17 showed the chronoamperometry and the corresponding transmittance curve, at the beginning upon application the external voltage, the PAM ECDs showed a high current density due to the presence of many active species. As the concentration of active species gradually decreased, the current density also gradually decreased and finally stabilized. According to the linear plots of ΔOD versus Q_d plot (Fig. 3e and Fig. S16),[36] the CE values of PAM ECDs based on **DBP^{2+}2Br$^-$**, **DTMAPP^{4+}4Br$^-$** and **BTMAPP^{3+}3Br$^-$** were 96, 103 and 115 cm^2/C, respectively. Among them, the asymmetric viologen with a quaternary ammonium group, **BTMAPP^{3+}3Br$^-$** , had a higher CE value.

Table 1 Optical and electrochromic data of PAM ECDs based on **DBP^{2+}2Br$^-$**, **DTMAPP^{4+}4Br$^-$** and **BTMAPP^{3+}3Br$^-$**

Compounds	λ_{max} (nm)	ΔT_s (%)	ΔT_f after 16,000 s (%)	Retaining of the initial ΔT (%)	t_c (s)	t_b (s)	CE (cm^2/C)	PC (mW/cm^2)
DBP^{2+}2Br$^-$	550	42.3	29.9	70.7	7.65	6.75	96	0.444
DTMAPP^{4+}4Br$^-$	553	39.0	30.6	78.5	7.68	6.93	103	0.336
BTMAPP^{3+}3Br$^-$	550	43.5	41.6	95.6	7.52	9.24	115	0.372

The power consumption (PC) is an important parameter to evaluate the performance of electrical equipments. The PC value was calculated with P=UI by using the data from the transient distribution of current density and optical transmittance upon application of -1.2 V (Fig. S18). The PC values of PAM ECDs based on **DBP^{2+}2Br$^-$**, **DTMAPP^{4+}4Br$^-$** and **BTMAPP^{3+}3Br$^-$** were calculated as 0.444, 0.336 and 0.372 mW/cm^2, respectively. Compared to some liquid-state ECDs,[37,38] all the three PAM hydrogel-state ECDs showed a lower PC, this makes them have promising prospects in the fields of electrical equipment such as smart windows, electronic labels, displays, etc.

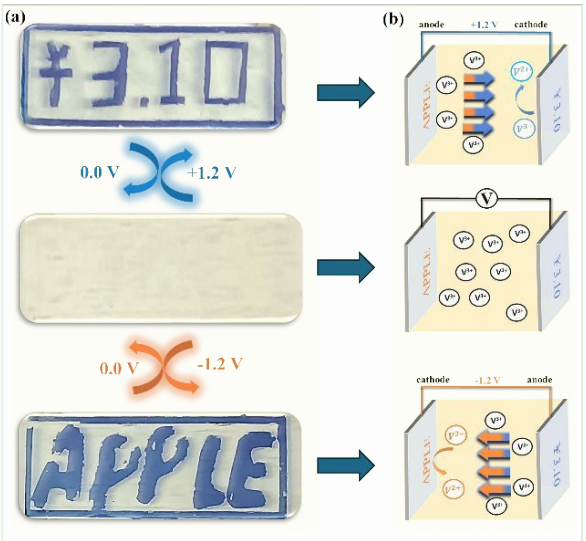

Fig. 4. Photographs (a) and schematic structure (b) of an electronic label based on **BTMAPP^{3+}3Br$^-$**.

Compared with other viologen (Table 2), the PAM ECD based on **BTMAPP^{3+}3Br$^-$** with asymmetric structure and a quaternary ammonium group showed a low working voltage, moderate optical contrast and response time, moderate coloration efficiency, good cycling stability, and ultra-low power consumption, which makes it has great development prospects in fields of energy conservation (such as: smart windows, electronic labels, displays, and so on).[14,15,25,28,32,39]

According to the method shown in Scheme S3, an electronic label based on **BTMAPP^{3+}3Br$^-$** was assembled. The electronic label could display three different states. When no voltage was applied (0.0 V), the label didn't display any pattern; when a voltage of -1.2 V was applied, the device displayed a pattern of "APPLE" (trade name); and when a voltage of 1.2 V was applied, the device displayed a pattern of "¥3.10" (trade price) (Fig. 4a). The reason is that **BTMAPP^{3+}3Br$^-$** is a cathodic ECM, which is reduced to discoloration at the cathode. When a voltage of 1.2 V is applied, "¥3.10" is the cathode, showing a pattern of "¥3.10"; when a voltage of -1.2 V is applied, the positive and negative electrodes are flipped, and "APPLE" is the cathode, showing the pattern of "APPLE" (Fig. 4b). This device can adjust the display information of electronic labels by controlling the applied voltage, it shows a great potential prospect in the field of electronic labels.

View Article Online
DOI: 10.1039/D5NJ02611C

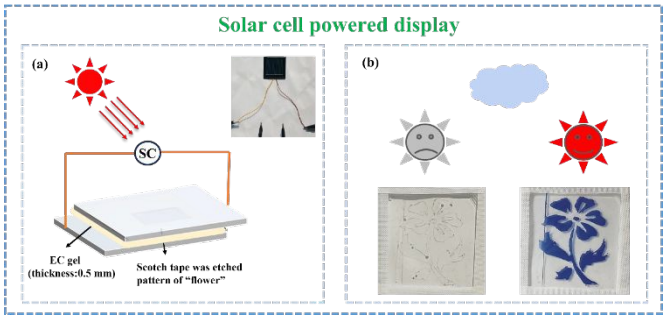

Fig. 5. Structure (a) and photographs (b) of a solar panel powered display based on **BTMAPP^{3+}3Br^{-}.**

View Article Online
DOI: 10.1039/D5NJ02611C

ARTICLE

Table 2 Electrochromic properties of the PAM ECD based on **BTMAPP^{3+}3Br^{-}** compared with some ECDs based on other viologen

Electrolyte matrix/ECMs [a]	Applied voltage (V)	ΔT (%)	t_c/t_b (s)	Retaining of the initial ΔT (%)	CE (cm^2/C)	Ref. No
PAM hydrogel/ **BTMAPP^{3+}3Br^{-}**	-1.2	43.5	7.52/9.24	72.4% after 1800 cycles	115	This work
DMSO/DBBP	-1.4	25	1.43/0.74	64% after 1000 cycles	95	14
[BMI][BF_4]/BHV(PF_6)$_2$	-1.2	42	-[b]/10.6	82% after 500 cycles	123.4	15
PVA-borax hydrogel/ $DHPV^{2+}2Cl^-$	-1.0	62	4.5/2.1	25% after 5000 cycles	165	25
PVB gel/ $DHPV^{2+}2Cl^-$	-1.0	51	5.6/5.3	98% after 10000 cycles	301	25
PAM hydrogel/V-OHP	-1.4	65.1	10/33	over 94% after 800 cycles	–[b]	28
PVA gel/BBV	1.3	71.33	3.9/7.4	82.66% after 10,000 cycles	102.62	32
(PVDF-co-HFP)+ionic liquid/ MHV-H	-1.3	65	8/75	77% after 1200 cycles	94.5	39

[a] DBBP: 1,1'-dibutyl-(4,4'-bipyridine)-1,1'-diium; BHV(PF_6)$_2$: 1-benzyl-1'-heptyl-4,4'-bipyridinium salt; $DHPV^{2+}2Cl^-$: 1,1'-bis(2,3-dihydroxypropyl) viologen dichloride; V-OHP: 1,1'-bis(3-hydroxypropyl) viologen dibromide; BBV: benzyl boronic acid viologen; MHV-H: monoheptyl viologen hexafluorophosphate
[b] no reported

As energy sources are increasingly depleted, natural resources such as solar energy has become an important part of energy conservation. A solar panel powered display based on **BTMAPP^{3+}3Br^{-}** was assembled, the structure was shown Fig. 5a, a "flower" pattern was etched on one piece of ITO-coated glass. When there is no sunlight, the device is in colorless bleached state due to no electric supply, while a "flower" pattern is clearly displayed upon sunlight irradiation because the solar panel provides the electric supply (Fig. 5b).

To investigate the application prospect of PAM ECD based on **BTMAPP^{3+}3Br^{-}** in smart windows, a large area ECD (8 × 8 × 0.05 cm^3) was assembled, and the photographs of ECD in the bleached and colored states were shown in Fig. 6a. Compared to the colored state of a smaller size ECD (3 × 3 cm^2, blue-purple), the large size ECD showed a blue coloration, the color discrepancy may be attributed to different concentration of cation radical. In fact, color discrepancy was also observed in previous reports when the size of electrochromic device is different.[2,25] The building behind the large area ECD can be clearly observed in both bleached (0.0 V) and colored states (-1.5 V) (Fig. 6b), this indicates that it can be applied in the field of smart windows. To verify its application in the field of smart windows, the ECD was used as the smart window of a home-made styrofoam box (20.5 × 10.7 × 13.2 cm^3) with an infrared lamp as the heating source, the temperature change in the box was monitored with a temperature detector when the ECD was in both bleached and colored states (Fig. 6c). The temperature difference between the bleached and colored states was 2.5°C (Fig. 6d), showing good thermal insulation, cooling effect and temperature adjustment. Therefore, this smart window shows promising prospects in energy-saving fields.

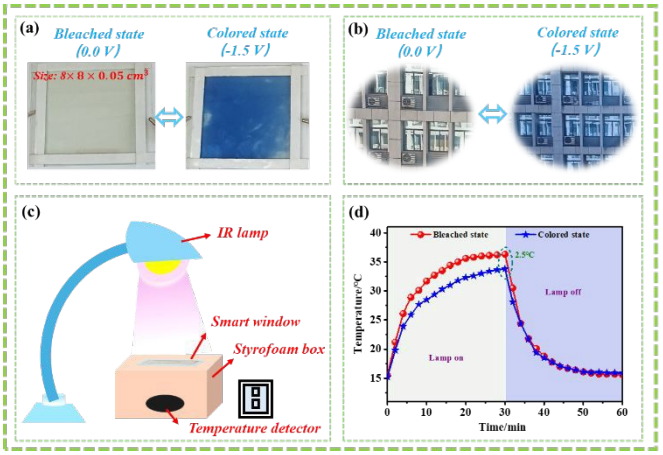

Fig. 6. Photographs of a large-area PAM ECD based on **BTMAPP^{3+}3Br^{-}** in the bleached and colored states (a), viewed from the inside to the outdoors (b), the model of smart window (c) and the temperature profiles in bleached state and colored state with IR light on and off (d).

Although the PAM ECD based on **BTMAPP^{3+}3Br^{-}** showed good cycling stability, its electrochromic performance still needs to improve for real application. As the cycling stability of hydrogel-state ECDs is highly dependent on ECM and electrochromic hydrogel matrix, introducing π-spacer between two pyridines of asymmetric viologens or introducing double-network hydrogel may further enhance the electrochromic performance,[2,14,18] this will also be the direction of our future efforts.

Experimental

Materials and methods

4,4'-Bipyridine (AR, 98%), 1-bromobutane (AR, 98%), AM (AR, 99%), *N,N'*-methylenebisacrylamide (MBAA, AR, 99%), 2-hydroxy-4'-(2-hydroxyethoxy)-2-methylpropiophenone (AR, 98%), 3-bromopropyltrimethylammonium bromide (AR, 99%) and lithium chloride (AR, 99%) were purchased from Shanghai Aladdin Co., P. R. China. 1,1'-Ferrocenedimethanol ($Fc(CH_2OH)_2$, AR, 98%) was purchased from Shanghai DiBai Co., P. R. China. Unless otherwise specified, the reagents were used directly.

^{1}H and ^{13}C NMR were measured on a Bruker AV 600 (600 MHz) spectrometer (Germany). High-resolution mass spectra (HRMS) were measured on a Bruker Impact Ⅱ instrument (Germany). The electrochemical impedance spectroscopy (ESI), cyclic voltammetry (CV) and linear scanning voltammetry (LSV) were measured on a CHI 650B electrochemical workstation (Shanghai Chenghua). The electrochromic performance was measured on a Shimadzu UV-2700 spectrophotometer (Japan) and RST5060F electrochemical workstation (Zhengzhou Shirui). ITO-coated glass (surface resistance 7-10 Ω/sq) was purchased from Wuhu Token Sciences Co., Ltd, P. R. China. The chromaticity coordinates (L*a*b*) value was obtained on a CR-10 plus (Konica Minolta, Inc., Japan) color reader.

Synthesis of ECMs

BTMAPP^{3+}3Br^{-}, **DTMAPP^{4+}4Br^{-}** and **DBP^{2+}2Br^{-}** were synthesized according to N-alkylation reaction by controlling the reaction conditions. The detailed synthesis process and characterization were shown in Supporting Information.

Preparation of PAM hydrogel

AM (5.00 g, as the monomer), MBAA (0.05 g, as the cross-linking agent, 1.00 wt.% of AM), 2-hydroxy-4'-(2-hydroxyethoxy)-2-methylpropiophenone (0.06 g, as the initiator, 1.20 wt.% of AM) and different LiCl concentrations were dissolved in deionized water to make a 20 mL solution. Among them, the concentrations of LiCl were 0.05, 0.10, 1.00, 2.00, 3.00 and 4.00 mol/L, respectively. The precursor solution was polymerized for 30 min under irradiation at 365 nm with a 20 W UV light, resulting in PAM hydrogels with different LiCl concentrations, which were denoted as PAM_1, PAM_2, PAM_3, PAM_4, PAM_5 and PAM_6, respectively.

Construction of hydrogel-state electrochromic devices

ECM (10 mmol/L) and $Fc(CH_2OH)_2$ (10 mmol/L, as complementary redox species) were added to the precursor solution of PAM_4, and the mixture was stirred till the formation of a faint yellow precursor solution. The PAM ECD with an effective area of 3 × 3 cm^2 was fabricated by dropping the precursor solution between two ITO glass electrodes separated by scotch tape (thickness: 0.1 mm), and then polymerized for 1 h under UV light. The assembly process was shown in Scheme S2.

Conclusions

In summary, an asymmetric disubstituted viologen with two different N-substituents and a quaternary ammonium group (**BTMAPP^{3+}3Br^{-}**) and two symmetric disubstituted viologen (**DTMAPP^{4+}4Br^{-}** containing two quaternary ammonium groups; **DBP^{2+}2Br^{-}** without quaternary ammonium group) were synthesized as the ECMs. PAM hydrogel-state ECDs based on three ECMs were assembled by in-situ photo-initiated polymerization of the monomer acrylamide under UV light, this easy procedure avoids the problem of forming bubbles. All three PAM ECDs required a same working voltage and achieved a similar color change from colorless bleached state to blue-purple colored state. As expected, the PAM ECD based on **BTMAPP^{3+}3Br^{-}** showed a better cycling stability (retaining of the initial optical contrast after 16,000 s monitored at a special wavelength between -1.2 V and 0.0 V: 95.6% versus 70.7% and 78.5%) and a higher coloration efficiency (115 cm^2/C versus 96 cm^2/C and 103 cm^2/C) compared to the PAM ECDs based on two symmetric disubstituted viologen. The results indicate that an asymmetric disubstituted viologen containing a quaternary ammonium group can enhance the cycling stability of the hydrogel-state ECD through suppressing the formation of radical cation dimers. The all-in-one semi-solid hydrogel-state ECD based on **BTMAPP^{3+}3Br^{-}** with advantages of easy-to-make process, good cycling stability, low operating voltage, high coloration efficiency and low power consumption offers a new choice for electronic labels, displays, smart windows, etc.

Conflicts of interest

There are no conflicts to declare.

Acknowledgements

The authors thank financial support from Chongqing Municipal Education Commission (Grant No. CY240224 and CY240225) and College Students' Innovation and Entrepreneurship Training Program (Grant No. S202410635097).

Notes and references

1 J. N. Liu, Q. He, M. Y. Pan, K. Du, C. B. Gong, Q. Tang, *J. Mater. Chem. A*, 2022, **10**, 25118-25128.
2 F. Y. Sun, H. Zhang, C. Wang, H. Ling, J. Cai, W. L. Peng, Y. H. Tian, F. Y. Su, Y. Q. Tian, Y. J. Liu, *Mater. Chem. Phys.*, 2023, **301**, 127593.
3 J. K. Wang, Z. P. Wang, M. Zhang, X. T. Huo, M. Guo, *Chem. Eng. J.*, 2024, 484, 149628.

4 H. Zhang, F. Y. Sun, J. Y. Feng, H. Ling, D. Y. Zhou, G. Cao, S. Wang, F. Y. Su, Y. Q. Tian, Y. H. Tian, *Cell Rep. Phys. Sci.*, 2022, **3**, 101193.
5 R. T. Song, G. P. Li, Y. Y. Zhang, B. Rao, S. X. Xiong, G. He, *Chem. Eng. J.*,2021, **422**, 130057.
6 Y. Y. Wang, C. X. Lei, W. X. Guan, K. Wu, B. W. Zhang, G. H. Yu, *Adv. Mater.*, 2024, **36**, 2403499.
7 J. H. Wang, L. Zhang, W. Zhan, J. H. Dong, Y. X. Ma, J. Li, W. J. Li, C. Zhang, *Chem. Eng. J.*, 2024, **483**, 149078.
8 J. N. Liu, K. Du, J. H. Guo, D. Wang, C. B. Gong, Q. Tang, *Small*, 2024, **20**, 2311823.
9 H. C. Peng, H. B. Wang, Y. P. Wang, X. Wang, S. Chen, B. Yan, *J. Mater. Chem. A*, 2022, **10**, 20302-20311.
10 C. H. Du, H. Li, G. Zhang, R. T. Wan, W. Y. Zhang, X. J. Xu, L. Zheng, X. K. Deng, J. K. Xu, B. Y. Lu, G. M. Nie, *Chem. Eng. J.*, 2024, **495**, 153692.
11 C. J. Schoot, J. J. Ponjee, H. T. Vandam, R. A. Vandoorn, P. T. Bolwijn, *Appl. Phys. Lett.*, 1973, **23**, 64-65.
12 F. Feng, S. Guo, D. Y. Ma, J. M. Wang, *Sol. Energy Mater. Sol. Cells*, 2023, **254**, 112270.
13 K. Madasamy, D. Velayutham, V. Suryanarayanan, M. Kathiresan, K. C. Ho, *J. Mater. Chem. C*, 2019, **7**, 4622-4637.
14 Z. J. Huang, F. Li, J. P. Xie, H. R. Mou, C. B. Gong, Q. Tang, *Sol. Energy Mater. Sol. Cells*, 2021, **223**, 110968.
15 M. Kim, Y. M. Kim, H. C. Moon, *RSC Adv.*, 2020, **10**, 394-401.
16 B. Ambrose, R. P. Naresh, M. Ulaganathan, P. Ragupathy, M. Kathiresan, *Mater. Lett.*, 2022, **314**, 131876.
17 E. S. Beh, D. De Porcellinis, R. L. Gracia, K. T. Xia, R. G. Gordon, M. J. Aziz, *ACS Energy Lett.*, 2017, **2**, 639-644.
18 M. Y. Pan, Q. He, J. N. Liu, K. Du, C. B. Gong, Q. Tang, *Dyes Pigm.*, 2023, **212**, 111126.
19 F. Y. Sun, J. Y. Cai, H. B. Wu, H. Zhang, Y. H. Chen, C. W. Jiang, F. Y. Su, Y. Q. Tian, Y. J. Liu, *Sol. Energy Mater. Sol. Cells*, 2023, **260**, 112496.
20 L. Ma, S. Xiao, N. Wu, S. Zhao, D. B. Xiao, *Dyes Pigm.*, 2019, **168**, 327-333.
21 M. J. Chang, W. N. Chen, H. D. Xue, D. L. Liang, X. F. Lu, G. Zhou, *J. Mater. Chem. C*, 2020, **8**, 16129-16142.
22 S. X. Xiao, Y. J. Zhang, L. Ma, S. Zhao, N. Wu, D. B. Xiao, *Dyes Pigm.*, 2020, **174**, 108055.
23 L. Yin, X. L. Yan, C. X. Yang, C. B. Gong, Q. Tang, *Dyes Pigm.*, 2024, **231**, 112419.
24 Y. J. Zhang, X. J. Shi, S. X. Xiao, D. B. Xiao, *Dyes Pigm.*, 2021, **185**, 108893.
25 S. Zhao, W. D. Huang, Z. S. Guan, B. Jin, D. B. Xiao, *Electrochim. Acta*, 2019, **298**, 533-540.
26 T. J. Adams, A. R. Brotherton, J. A. Molai, N. Parmar, J. R. Palmer, K. A. Sandor, M. G. Walter, *Adv. Funct. Mater.*, 2021, **31**, 2103048.
27 M. J. Chang, D. L. Liang, F. Zhou, H. D. Xue, H. Zong, W. N. Chen, G. Zhou, *ACS Appl. Mater. Interfaces*, 2022, **14**, 15448-15460.
28 Z. Tajmoradi, H. Roghani-Mamaqani, K. Asadpour-Zeynali, M. Salami-Kalajahi, *Microchem. J.*, 2024, **207**, 111698.
29 Y. H. Ye, Y. F. Zhang, Y. Chen, X. S. Han, F. Jiang, *Adv. Funct. Mater.*, 2020, **30**, 2003430.
30 X. Y. Zhang, Z. K. Han, T. L. Cao, Y. Zhu, Z. G. Wang, Z. Y. Zhang, Z. Y. Zhao, D. Q. Zhang, N. Yan, Y. Y. Zhang, G. He, *Chem. Eng. J.*, 2025, **503**, 158494.
31 Q. J. Chen, J. X. Zhao, J. M. Zheng, C. Y. Xu, *Electrochim. Acta*, 2022, **431**, 141156.
32 S. W. Tang, R. Z. Zheng, J. L. Niu, Z. Q. Wan, C. Y. Jia, X. L. Weng, L. J. Deng, *Sol. Energy Mater. Sol. Cells*, 2023, **257**, 112353.
33 M. A. Ochieng, J. F. Ponder, J. R. Reynolds, *Polym. Chem.*, 2020, **11**, 2173-2181.
34 H. Oh, J. K. Lee, Y. M. Kim, T. Y. Yun, U. Jeong, H. C. Moon, *ACS Appl. Mater. Interfaces*, 2019, **11**, 45959-45968.
35 D. Y. Ma, G. Y. Shi, H. Z. Wang, Q. H. Zhang, Y. G. Li, *J. Mater. Chem. A*, 2014, **2**, 13541-13549.
36 D. Y. Ma, G. Y. Shi, H. Z. Wang, Q. H. Zhang, Y. G. Li, *J. Mater. Chem. A*, 2013, **1**, 684-691.
37 M. Y. Pan, Q. H. Zhou, J. N. Liu, Q. He, C. B. Gong, Q. Tang, W. Shen, *Sol. Energy Mater. Sol. Cells*, 2022, **240**, 111712.
38 Q. H. Zhou, K. Du, L. Qiang, J. H. Guo, Q. He, Y. Wu, Q. Tang, W. Shen, C. B. Gong, *Dyes Pigm.*, 2023, **219**, 111645.
39 T. Y. Yun, H. C. Moon, *Org. Electron.*, 2018, **56**, 178-185.

View Article Online
DOI: 10.1039/D5NJ02611C

Data availability statement

The main experimental data are provided within the main text and the ESI.